Photochemical delivery of nitric oxide.

Peter C. Ford

Department of Chemistry and Biochemistry, University of California, Santa Barbara
Santa Barbara, CA 93106-9510 USA; EMAIL: ford@chem.ucsb.edu

Abstract:

There remains considerable interest in developing methods for the targeted delivery of nitric oxide and other small molecule bioregulators such as carbon monoxide to physiological targets. One such strategy is to use a "caged" NO that is "uncaged" by excitation with light. Such photochemical methods convey certain key advantages such as the ability to control the timing, location and dosage of delivery, but also have some important disadvantages, such as the relatively poor penetration of the ultraviolet and visible wavelengths often necessary for the uncaging process. Presented here is an overview of ongoing studies in the author's laboratory exploring new photochemical NO precursors including those with nanomaterial antennas designed to enhance the effectiveness of these precursors with longer excitation wavelengths.

Keywords: nanomaterial, quantum dot, photochemistry, photoCORM, upconversion.

Introduction:

The purpose of this article is to provide an overview of studies in my laboratory relevant to the delivery of small molecule bioregulators to physiological targets. Our approach and that of others to more controlled, specific delivery is to develop stable compounds that release the molecule in question only when triggered by an external signal, namely photo-excitation of an appropriate precursor. The precursor is in principle inactive, hence the bioactive agent of interest is "caged", but upon photoexcitation, the latter species is released ("uncaged") (Scheme 1). Although we have focused primarily on the delivery of nitric oxide [1-3], these strategies should apply to other chemotherapeutic molecules such as carbon monoxide, which has also drawn our recent attention [4-6]. For CO, the term "photoCORM" (for photoactivated CO releasing moiety) has been coined [4] to designate a photochemical CO precursor, and, while no such term has caught on with NO precursors, one now hears "photoNORM" used occasionally. The advantage of photo-activation is that the external signal allows one to define the *location* and *timing* of the NO delivery. Furthermore, since the amount of photochemical reaction is a function of the quantity of light delivered to the desired target, this allows one also to define the *dosage* of the release. Although the present manuscript is focused largely upon our own studies, it should be noted that there is a growing interest in applying photochemical methods to the uncaging of NO [7-12] and CO [5,13-14] as well as other bioregulators [15].

Scheme 1: Cartoon illustrating the photochemical uncaging of a bioactive substance which in the original "caged" form (presumably some type of conjugate) is not active.

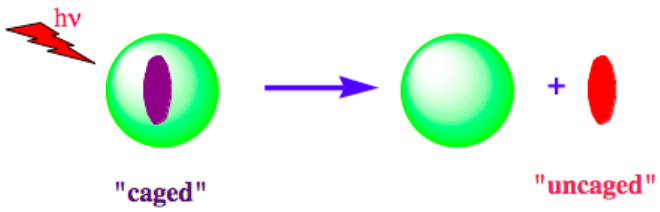

Various rationales for controlled NO delivery range include its cardiovascular effects, antibacterial properties and potential roles in generating apoptosis in tumor cells. With regard to cancer therapy, one problem is that, although high localized levels of NO can induce cell apoptosis, low levels of NO may induce tumor growth instead [16]. Thus, it is essential to have very careful control over the dosage delivered. In this context our interest in the phototherapeutic NO delivery draws from the view that this should be synergistic with other

forms of treatment. For example, it has been shown that NO increases the sensitivity of tumor cells to radiation therapy [17] and chemotherapy [18]. The hypoxic regions of malignant tumors are much more radio-resistant than is normoxic tissue, therefore one should be able to reduce the collateral damage from radiotherapy by developing strategies to increase the sensitivity of the targeted tissue. Hypoxia radiation resistance may be alleviated by introducing a sensitzer and/or a vasodilator to increase tissue oxygenation; both are roles played by NO. Radiation sensitization requires NO concentrations near 1 μM [17], but vasodilation is triggered at much lower concentrations of NO [19], so that even at very low concentrations, exogenously delivered NO may indirectly enhance the radiation killing of tumor tissue.

An example of such radiation sensitization is illustrated in Figure 1. In this case, four different samples of V-79 (Chinese hamster lung fibroblast cells) were subjected to γ-radiation from a Co-60 source in an equivalent manner and the resulting cell viability evaluated [20]. One cell sample was under aerobic conditions, and it is easily seen that less than 1% of the cells were stlll viable after a γ-radiation dose of ~11 Gy. In contrast, hypoxic cells proved to be much more resistant, with radiation doses exceeding 25 Gy to achieve a comparable effect. The same cells incubated with a 500 μM solution of the photochemical NO donor Roussin's red salt $Na_2[Fe_2S_2(NO)_4]$ (RRS, see below) showed no enhancement of the radiation effect, but when a

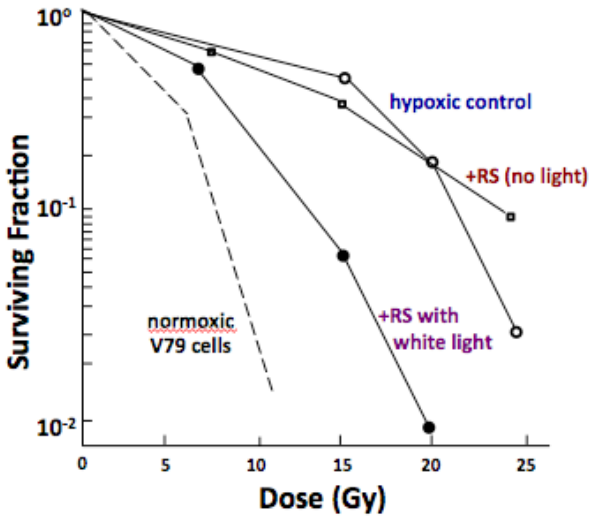

Figure 1. Survival of V79 Chinese hamster lung cells exposed to γ-radiation under hypoxic conditions without (open circles) or with 500 mM Roussin's red salt (RS) under simultaneous irradiation with white light (closed circles) or in the dark (open squares). The dashed line on the plot indicates the response of V79 cells exposed to γ-radiation under normoxic conditions (WL refers to white light illumination. (Adapted with permission from ref. 20 Copyright 1997 American Chemical Society.)

comparable sample was also illuminated with light from a simple 35 mM projector, a marked enhancement of the radiation damage was apparent. Given that these results paralleled those observed when other NO donors were utilized, it was concluded that the photochemical release of NO from the RRS is responsible for the observed sensitization [20].

With regard to carbon monoxide, it has long been known that CO is produced endogenously by heme oxygenases, and there are newer developments indicating that endogenously and/or exogenously produced CO may be cytoprotective during inflammation, promote wound healing, and have signaling properties [for examples: 21-22]. In addition various CO donors have been shown in animal studies to be effective in alleviating ischemia/reperfusion (I/R) injury in various organs and tissues [for examples: 23-25].

Strategies for and problems with developing methodologies for photochemical CO and NO release show certain parallels. One property desirable for a photochemical precursor would be solubility in aqueous solution or (perhaps) in a medium such as aqueous dimethylsulfoxide (DMSO) that is commonly used for drug delivery. Another would be reasonable stability in aerated aqueous media at physiological temperatures and other conditions typical to living organisms. A third would be photoreactivity at wavelengths where the transmission of light is optimal (Figure 2) [26]. Penetration depth of light into tissue is strongly wavelength dependent.

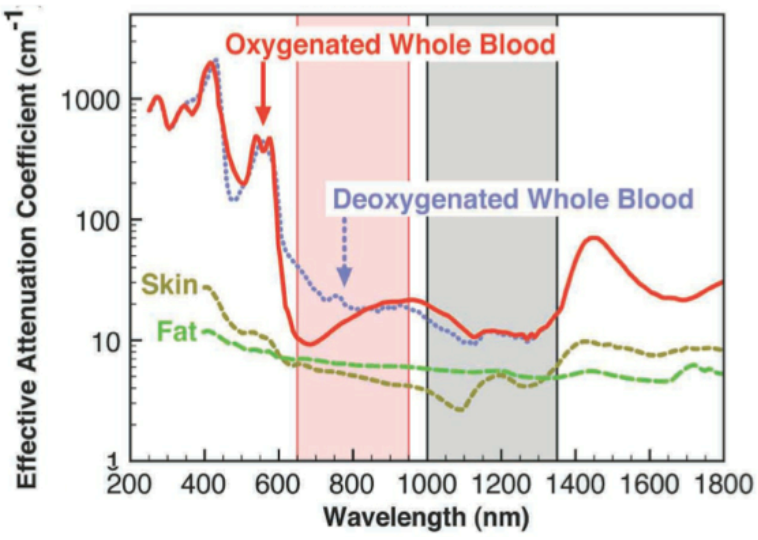

Figure 2: Absorption properties of various tissue components showing the windows in the near-infrared spectral region (adapted from ref. 26 with permission from the Nature Publishing Group. Original figure provided by Dr. A. Smith of Emory University)

It is shallow for ultraviolet light, but improves for longer visible wavelengths and tissue penetration reaches its deepest values in the near infrared (NIR) spectral region (~700-1100 nm).

Photochemical activation at these longer wavelengths might be accomplished by using antenna chromophores having high extinction coefficients at the desired wavelengths (Scheme 2). However, such an antenna can be an effective photosensitizer only if there are acceptor states on the precursor molecule having the appropriate energies. A more ambitious approach would be to utilize an antenna with a high two-photon excitation (TPE) cross-section in the NIR. For such a system, excitation with a NIR laser could generate high-energy photosensitizer states that can access reactive excited states of the photochemical precursor. We will discuss this approach below.

It should be noted that, while these photochemical precursors are designed to release the caged bioactive substance upon irradiation with light, a remaining molecular fragment is also produced. These should be identified and characterized along with any secondary products readily formed by subsequent reaction with the medium. Furthermore, the physiological properties of these other photoproducts need to be examined to confirm whether the perceived physiological effect is due to release of the caged species or to the unforeseen activity of other species directly or indirectly generated. Lastly, as in the development of any new therapeutic strategy, the acute and long-term toxicity of all these compounds must be evaluated.

Scheme 2. Single- or two-photon excitation of an antenna/photochemical precursor conjugate leading to release of XY (CO or NO). D is the donor molecule acting as an antenna to absorb light give an excited state D* that undergoes energy transfer to the acceptor molecule L_xM-XY, which is represented here as a metal complex that releases X-Y after the energy transfer step.

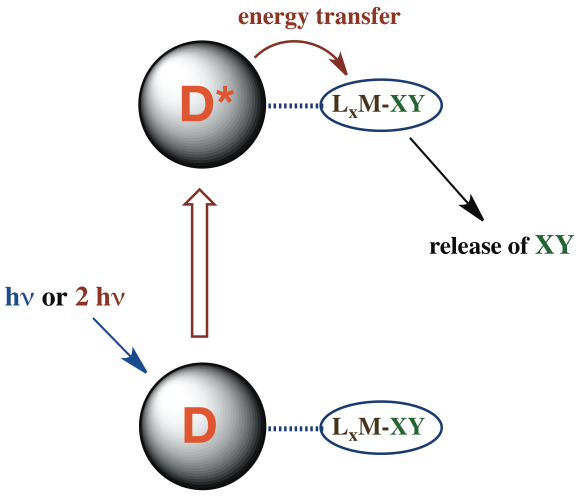

In photochemical research, the efficiency noted above is called the *quantum yield* (Φ_P, eq. 1), which is the amount (in moles) of the desired chemical reaction ΔP per Einstein of light absorbed $\Delta h\nu$ (one Einstein = 6.023×10^{23} photons) by the photoactive precursor (eq. 1).

$$\Phi_P = \Delta P/\Delta h\nu \quad (1)$$

For single photon excitation (SPE), ΔP should be a linear function of $\Delta h\nu$. Generally Φ_p is determined for photoexcitation at a specific wavelength, since it may be wavelength dependent.

When the goal is to perturb a dynamic physiological system by photochemical release of a bioactive substance, the uncaging *rate* may be of greater interest. This is defined by (eq. 2),

$$d[P]/dt = \Phi_P I_a \quad (2)$$

where d[P]/dt is the rate product formation in moles per unit time per unit volume and $I_{\square}$ is the intensity of the light absorbed by the precursor in Einsteins per unit time per unit volume at the excitation wavelength. $I_{\square}$ is a function both of the incident light intensity I_o and the ability of the compound to absorb at the wavelength of excitation. For a solution phase system where the photoreactant is the only species absorbing the incident light,

$$I_{\square} = I_o(1\text{-}10^{-Abs(\lambda)}) \quad (3)$$

where $Abs(\lambda)$ is the solution absorbance at the excitation wavelength λ_{irr} and equals the product of the molar concentration of the photoactive species (c), the molar extinction coefficient (ε_λ, in L moles^{-1} cm^{-1}) at the wavelength λ and the path-length of the solution cell (in cm). Thus, the rate of photoproduct formation under SPE at a particular wavelength will be directly proportional to I_0 and to Φ_P and will be a more complex function of c and ε_λ. In this context, efficient photochemical delivery to physiological targets should be more favorable with precursors that absorb strongly at the desired excitation wavelength(s) λ_{ex}. If the product $c \times \varepsilon_\lambda$ is sufficiently large, all the light is absorbed and the photoreaction rate becomes independent of both terms. However, this scenario is unlikely in a targeted tissue, and absorption by other chromophores or scattering of the light beam can have a significant effect on I_a. When polychromic light is used, the photochemical rate is the integral of $\Phi_P \times I_a$ over the excitation wavelengths, noting that Φ_P may be, and I_a certainly will be, functions of λ_{irr}.

The ensuing sections will discuss first the use of typical single photon excitation methods with various nitric oxide precursors ("caged NO"), including those with antenna chromophores to enhance the absorption of light. We will then examine the potential applications of multi-photon excitation methods to facilitate the photochemistry of such precursors using tissue penetrating near infrared (NIR) light.

Photochemical NO precursors:

Scheme 3 illustrates several representative types of transition metal complexes that release NO upon photoexcitation. Two of these (a and b) are metal nitrosyls, where the nitric oxide is caged by coordination to a transition metal center [20,27]. For such complexes, a commonly observed photochemical process is cleavage of the metal-NO bond to give neutral NO (rather

Scheme 3. Examples of photochemical NO release from compounds representative of those under study. a. Roussin's red salt anion. b. A ruthenium salen nitrosyl complex. c. The Cr(III) nitrito complex *trans*-$Cr(cyclam)(ONO)_2^+$ (cyclam = 1,4,8,11-tetrazacyclotetradecane)

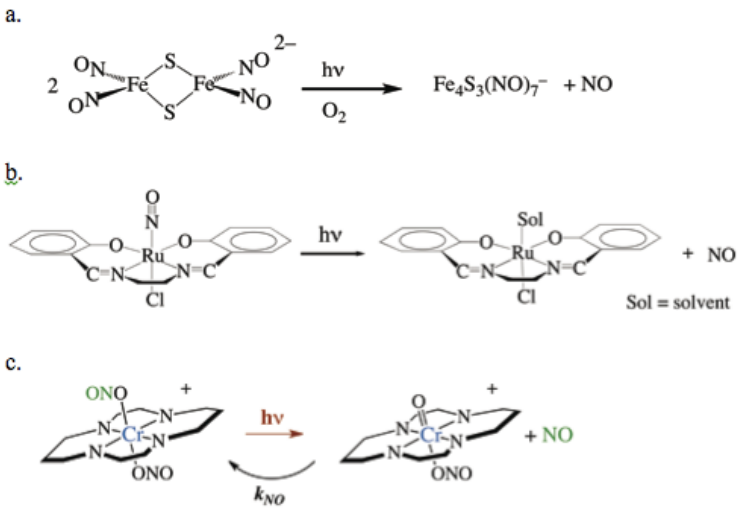

than the ionic species NO^- or NO^+). The third example is an O-nitrito complex [28] where the NO is caged by bonding to another oxygen. In this case, NO is released by homolytic cleavage of the MO-NO bond. Since the nitrogen of nitrite ion is formally in the +3 oxidation state and that of NO is formally +2, the extra electron must come from the metal center. Thus, for the example shown, the release of NO is accompanied by the oxidation of the metal, in this case a chromium(III).

The iron sulfur nitrosyl anionic cluster, Rousin's red salt anion (RRS) was the NO precursor used to demonstrate that photochemically released NO enhances the ability of γ-radiation to kill hypoxic cultured cells as illustrated in Figure 1. RRS absorbs broadly in the visible and this radiation sensitization experiment proved quite successful using a simple slide projector as the white light source. However, RRS is only modestly stable in aerobic aqueous media, so in search of more stable analogs, our studies turned to the red salt esters (RSE) that are prepared by the reaction shown in eq. 4.

RRS **RSE** (4)

These RSE, even with simple ligands such as a benzyl or ethyl group, qualitatively displayed greater stability as well as more efficient NO release, since photolysis in aerated aqueous solution led to the release of all four NO's (eq. 5) [29].

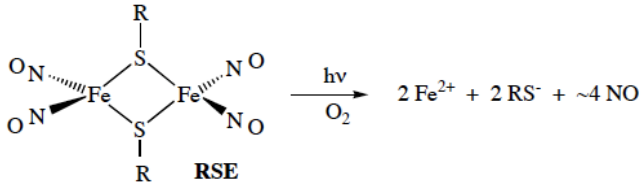

RSE (5)

Furthermore, variations of this synthetic procedure could be used to build RSE's with R-groups having strongly absorbing chromophores. Two such examples are PPIX-RSE and Fluor-RSE, where the pendant groups are derivatives of protoporphyrin XI [30] and of fluorescein [31], respectively. These pendant chromophores are much more efficient at gathering light than is the $Fe_2S_2(NO)_4$ cluster itself, hence they can serve as antennas that are first excited then undergo energy transfer to the cluster to photosensitize NO release.

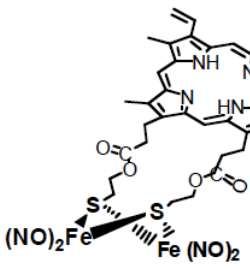

PPIX-RSE

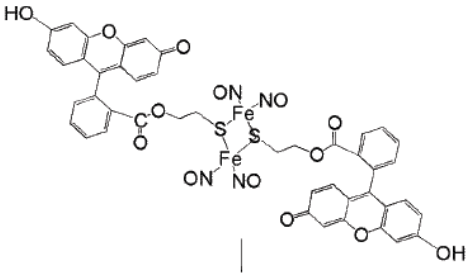

Fluor-RSE

The photochemistry of both PPIX-RSE and Fluor-RSE clearly demonstrate this antenna effect. For example, dilute solutions (10 μM), photo-decomposition of the PPIX-RSE conjugate excited at longer visible wavelengths (λ_{irr} 546 nm) occurred at much higher rates than did the simpler ester $Fe_2(\mu\text{-}SEt)_2(NO)_4$ (Et-RSE) under otherwise identical conditions [30]. The enhanced *rate* of NO release was largely attributed to the more efficient light absorption (I_a) by the tethered PPIX owing to the strong porphyrin Q-bands in this region. In addition, the fluorescence that is characteristic of the PPIX chromophore was largely quenched (Figure 3), presumably as the result of energy transfer to the RRS cluster. Thus, attaching an antenna to the red salt cluster enhances *the rate* of NO production via the visible light photoreaction as intended. However, *the quantum yields* for both PPIX-RSE and Et-RSE are relatively low at this excitation wavelength.

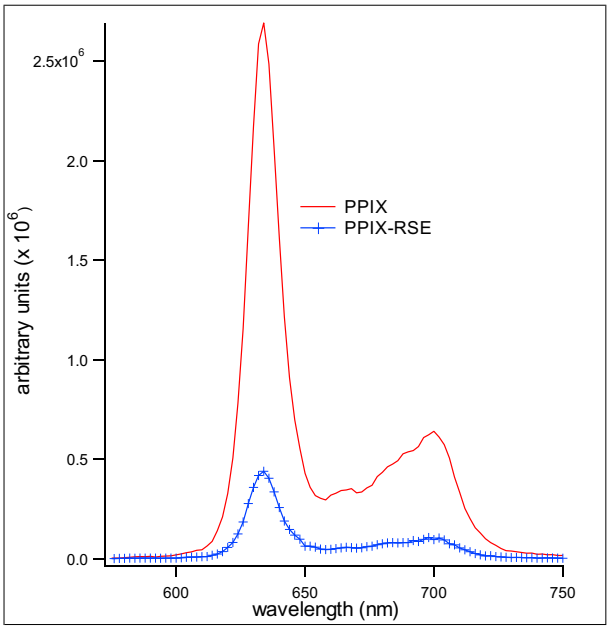

Figure 3. The fluorescence spectra of free PPIX and the red salt ester PPIX-RSE at comparable concentrations and under identical conditions, showing that the fluorescence from the latter is about 85% quenched by attachment to the Fe/S/NO cluster. Emission lifetime measurements confirm that this quenching is likely due to energy transfer to the cluster. (Reprinted with permission from ref 30. Copyright 2004, American Chemical Society.)

Fluor-RSE with two pendant fluorescein dye units represents the second generation of such Roussin's esters. This compound is moderately soluble in buffered aqueous solutions, and like PPIX-RSE, the characteristic fluorescence of the antennas is ~85% quenched upon linking to the Fe/S/NO cluster. The photochemistry of Fluor-RSE in aqueous media parallels that seen for other esters. Consistent with eq. 5, all four NOs were released with a Φ_{NO} of 0.014 when irradiated at 436 nm [31].

The metal nitrito complex *trans*-Cr(cyclam)$(ONO)_2^+$ (called "CrONO" in our lab) has several attractive features as a potential therapeutic photochemical NO precursor. First, it is thermally stable under physiologically relevant conditions (pH 7.4, normoxic aqueous buffer at 37 °C) and limited cell culture studies indicated no toxicity [32]. Second, CrONO is photoactive, and displays a substantial quantum yield for the release of NO according to the reaction shown in Scheme 3c over the wavelength range 365-536 nm. The quantum yield measured by spectral changes is 0.25-0.30 moles Einstein^{-1} and is essentially independent of the excitation wavelength λ_{ex}. Direct measurement of NO release using a Sievers Nitric Oxide Analyzer (NOA) gave an equivalent quantum yield ($\Phi_{NO} = 0.25$) when the trapping agent was GSH. However, the visible range absorption bands leading to this photochemistry are metal centered d-d bands (sometimes called ligand field bands) and these have very low extinction coefficients ε_λ, since they represent symmetry forbidden transitions. As a consequence, the rates of NO generation are relatively low unless the concentration of CrONO and/or the intensity of the excitation light source is high (see eqs. 2 and 3)

Another feature of the CrONO system is that there is a relatively fast back reaction ($k_{NO} = 3.1 \times 10^6$ M^{-1} s^{-1} in 298 K aqueous solution) to regenerate the coordinated nitrite [28]. In such a case, it may be necessary to trap the metal-containing fragment in order to ensure a substantial net yield of NO release. The $Cr^{IV}(O)$ intermediate formed by the reaction illustrated in Scheme 3c is subject to both oxidative and reductive trapping (Scheme 4) [32,33]. When either an oxidant such as O_2 or a reductant such as glutathione (GSH) is present to trap the Cr(IV) intermediate, permanent photochemistry is observed. Thus CrONO is an effective NO donor under a variety of conditions, but should be especially effective in hypoxic tissue where the Cr(IV) would be

Scheme 4: The reversible labilization of NO from CrONO. The net production of NO is effected by the trapping of the Cr(IV) intermediate by oxygen in aerobic media or by GSH in a more reducing environments. The reaction with O_2 in aerobic media is complicated by the formation of O_2^- which can trap a substantial fraction of the NO to give peroxoxynitrite (adapted from ref 33).

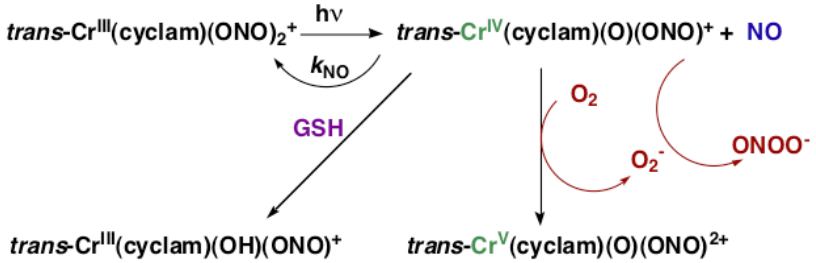

trapped by GSH or other reductants.

Despite the small molar extinction coefficients of CrONO, it is notable that the NO photochemically released from even quite dilute solutions is sufficient to activate the enzyme soluble guanylyl cyclase (s-GC) and to effect vasorelaxation in porcine arteries (Figure 4). Both phenomena, of course, reflect the great sensitivity of s-GC activation to NO [19]; nonetheless these observations demonstrate the potential applicability of the photochemical technique for delivering bioactive molecules to desired targets. For example, the experiments summarized by Figure 4 clearly show that the porcine arterial ring relaxation can be attributed to NO generated by photolysis of CrONO, not to other photoproducts nor to the complex itself. Under these conditions, the IC_{50} for solutions of CrONO is ~ 320 nM [33].

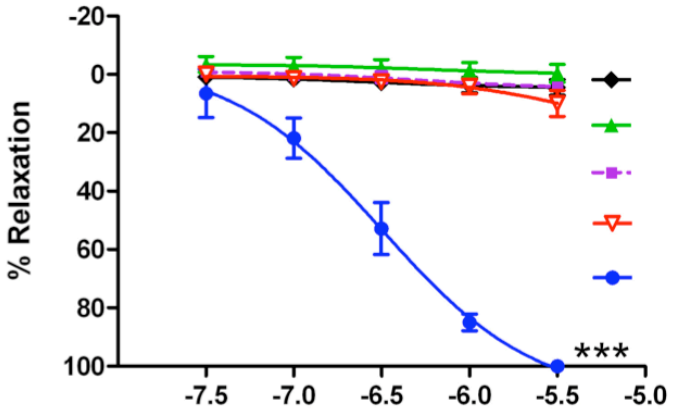

Figure 4: Effect of CrONO on vasorelaxation in endothelium-denuded porcine coronary arterial rings. Black diamonds: in the dark; Green triangles: ambient light; Blue circles: exposed to 470 nm LED; . Red open triangles: vasodilator effect of light activated CrONO was abolished the sGC inhibitor, ODQ is present. Purple squares: a product solution of photolyzed CrONO had no effect in the dark. (Figure adapted from ref. 33.)

Thus, CrONO is a compound that satisfies most criteria for a photochemical NO precursor with the exception of its very low absorptions at desired longer visible wavelengths. To address this limitation, we have therefore turned our efforts to attaching various chromophores to CrONO-like systems to serve as antennas for enhancing light absorption and increasing rates of photo-induced NO production. Our first studies in that regard focused on organic dyes linked via the macrocyclic cyclam ring, such as illustrated by Scheme 5 (top). Such conjugates clearly demonstrate that attachment of such a dye increases the rate of NO production from dilute solutions owing to the greater absorption cross sections of the pendant antenna [34].

Scheme 5. *Top:* Ilustration of a pendant pyrene type chromophore acting as an antenna to collect light and photosensitize the release of NO from a CrONO type center [32]. *Bottom:* Analogous photosensitization of NO release from CrONO using a water-soluble CdSe:ZnS core:shell semiconductor quantum dot as the antenna [34-36].

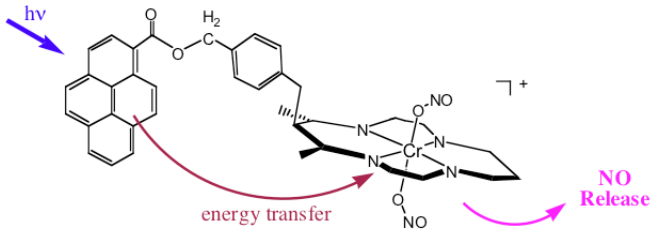

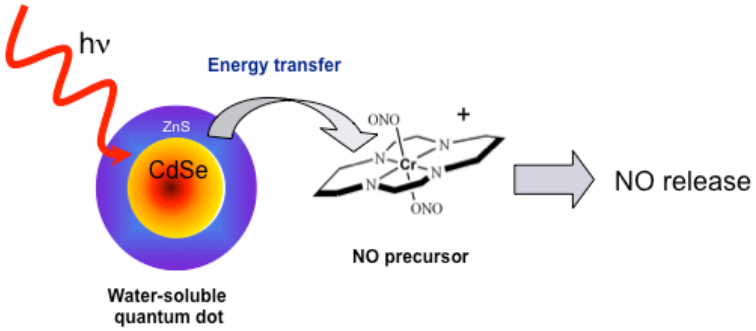

It was in this context that we decided to consider semiconductor quantum dots (QDs) as potential photosensitizers. The first system we explored consisted of CdSe:ZnS core:shell QDs with a core diameter of ~3.8 nm that had been ligand exchanged to decorate the surface with dihydrolipoic acid (DHLA) in order to impart water solubility at physiological pH [35,36]. In aqueous solution, these QDs displayed a photoluminescence (PL) centered at 570 nm, that was progressively quenched with increasing concentrations of added CrONO. More importantly, when a solution was prepared containing these QDs (100 nM) and CrONO (200 μM) and was photolyzed, substantially more NO was generated than from analogous solutions containing only CrONO at the same concentration. Subsequent studies confirmed that both the PL quenching and the sensitized NO production can be attributed to an energy transfer mechanism from the excited QDs to CrONO (Scheme 5 bottom) [36]. The interaction between the CrONO cations and the water-soluble QDs would appear to involve electrostatic assemblies formed by ion pairing at the anionic QD surfaces. We do not expect such assemblies to be stable under physiological conditions, hence we are developing synthetic protocols to attach CrONO and other photochemical nitric oxide precursors to the QD surfaces via strong covalent bonds.

Multi-photon excitation using near-infra red light.

The reactive excited states of otherwise attractive precursors are often too high in energy to be accessed by typical single photon excitation (SPE) using excitation at longer visible wavelengths or in the NIR therapeutic window. In such a case, even the attachment of an antenna with strong absorption bands does not help, since there would be insufficient energy to sensitize the population of these high energy states. In principle this limitation can be addressed by using multi-photon excitation, where the summed energy of several NIR quanta are sufficient to generate the energies necessary to trigger the desired uncaging. Two different multi-photon excitation approaches have been explored in our laboratory: (a) two photon excitation (TPE) which involves simultaneous absorption of two quanta of light, and (b) energy transfer upconversion (ETU) which can be obtained by sequential absorption processes. TPE is illustrated in Scheme 6, while ETU is discussed below

The rates of photochemical processes initiated by simultaneous or sequential multi-photon absorption processes typically will have a non-linear dependence on the light intensity I_o, which is different from the behavior of SPE stimulated processes (eqs. 2 & 3). For example, the probability of TPE is proportional to I^2, the square of the incident light intensity, if a single source is utilized. Thus, TPE induced photoreaction will be fastest at the focal plane of the light source. This therefore offers the possibility of 3-D spatial resolution, a property that is extensively exploited in imaging [37,38] and offers interesting possibilities in phototherapy [39].

Scheme 6. TPE model for achieving higher energy excited states (ES) using muti-photon excitation. TPE involves simultaneous absorption of two photons to generate an ES (E_2) having the summed energy of the two photons. The resulting ES may undergo emission, may react to give products or undergo energy transfer to another chromophore.

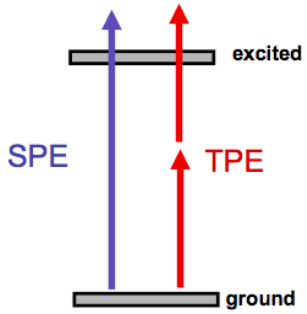

Two photon excitation and absorption: The selection rules for TPE are different from those for SPE; the former is allowed only between two states that have the same parity, while the latter

306 requires a parity change. Chromophores with high two photon absorption cross sections in the
307 NIR excitation region include extensively π-conjugated molecules especially that are
308 quadrupolar with electron-donor and -acceptor units arranged symmetrically with respect to the
309 center [40,41]. Semi-conductor quantum dots are also TPE chromophores with two photon
310 absorption cross sections as large as 10^4 GM seen for the commonly studied cadmium selenide
311 core or CdSe/ZnS core/shell QDs [42,43].[1]

312 Our first TPE study involved the Roussin's red salt ester PPIX-RSE that we had previously
313 shown to be photoactive to NO release when subjected to SPE at mid-visible wavelengths [29].
314 Wecksler et al tested this possibility by subjecting a solution of PPIX-RSE to 810 nm NIR
315 excitation with 100 fs pulses from a Ti/sapphire laser [44]. These intense NIR pulses led to weak
316 phosphorescence from PPIX-RSE (λ_{max} 632 nm) accompanied by NO generation. Both the NO
317 release and emission provided clear evidence that the higher energy ESs responsible for these
318 phenomena were being populated by multiphoton excitation, even though the two photon
319 absorption cross-section (δ) of PPIX is known to be quite low (~2 GM).

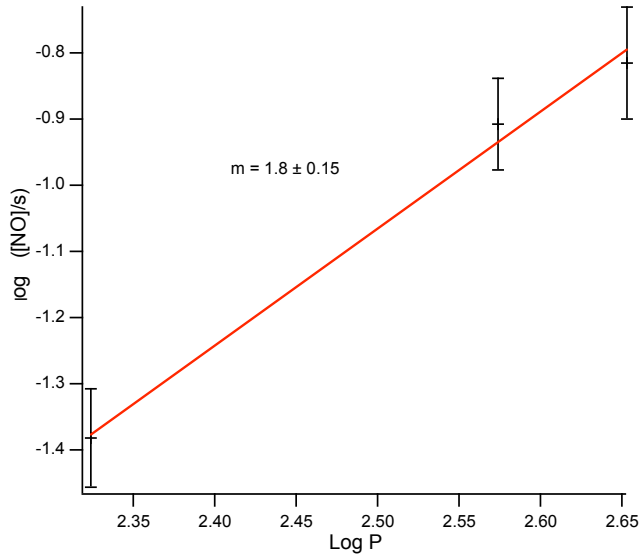

320

321 **Figure 5.** TPE of Fluor-RSE. Log [NO]/s versus Log *P* plot, where [NO]/s is the concentration of NO released in
322 30 s under 800 nm excitation, and *P* is the average power (in megawatts) of the pulsed laser (100 fs pulses at 80
323 MHz) which is proportional to the pulse intensity *I*. The slope = 1.8 ± 0.15. (adapted from ref. 31)
324

[1] The GM is the unit of two photon cross sections, and 1 GM = 10^{-50} cm^4 s photon^{-1}. This is named in honor of Maria Goeppert-Mayer, who first proposed theoretically the concept of two photon excitation, a concept that was not confirmed until decades later.

Wecksler extended these studies to two other red salt esters, Fluor-RSE and AFX-RSE. In both cases the pendant dyes have been shown to have much higher δ values [31,45]. In both cases, the fluorescence properties of the excited state species formed after TPE at 800 nm were the same as those observed upon SPE at 436 nm, indicated that the same states are formed regardless of the method of excitation. In each case, the fluorescence was markedly attenuated from that of analogous chromophores without the Fe/S/NO cluster, and this was accompanied by NO release. When Fluor-RSE was irradiated with 800 nm light from the ultrafast laser system, a log/log plot of the NO generated vs. the excitation intensity was linear with a slope of 1.8 ± 0.2 (Figure 5), consistent with the squared dependence on excitation intensity as expected for a photochemical process initiated by TPE [31].

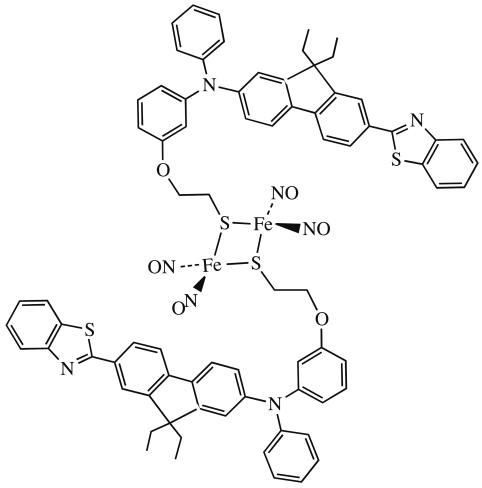

AFX-RSE

A subsequent study by Prasad and coworkers [46] described another RSE derivative $Fe_2(NO)_4(\mu\text{-}SR')_2$, where R'S- is the chromophore oligo-phenylene vinylene amine with a large δ, conjugated to tetra(ethylene glycol) ethers to improve aqueous solubility. Both SPE at 365 nm and TPE at 775 nm led to NO release as well as light dependent cytoxicity in Hela and Cos-7 cancer cell cultures. As expected the magnitude of the effect was greater in the SPE experiments owing to the greater flux of NO generated with direct UV excitation, although this advantage

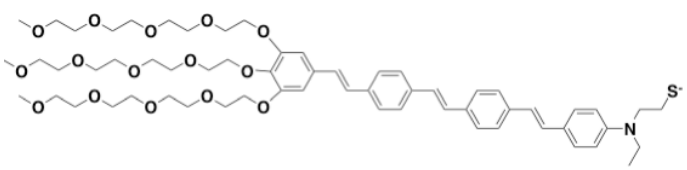

R'S$^-$

would be attenuated in tissue systems owing to the dramatically different transmission properties of the two wavelengths. This and the other studies with Roussin's red salt esters suggest the feasibility of using two photon excitation techniques for the delivery of NO to physiological sites, although much more needs to be done.

NO uncaging using Ln^{III}-doped NIR upconverting nanoparticles (UCNPs): Energy transfer upconversion (ETU) involving the sequential absorption of photons is another process that is nonlinear with regard to the intensity of the excitation source. Luminescent UCNPs based on the lanthanoid ions can be used in such devices owing to the relatively long lifetimes of the f-f excited states [47]. Typically, a Ln^{III} ion such as Yb^{3+} is the sensitizer that absorbs the NIR light and transfers this energy to an acceptor Ln^{III} ion such as Er^{3+}, Tb^{3+}, or Tm^{3+} as illustrated in Figure 6 [48]. Continued excitation of the sensitizer Yb^{3+} leads to further energy transfer to the long-lived acceptor states to populate new, higher energy states from which emission (or emissions) occurs at considerably shorter wavelengths than the initial NIR source. The absolute and relative intensities of the upconverted visible or ultraviolet wavelength emissions will depend nonlinearly on the intensity of the pumping process.

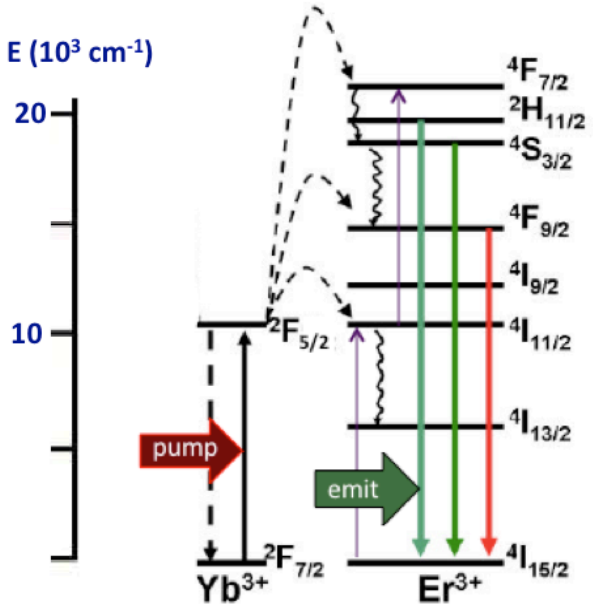

Figure 6. Energy transfer upconversion (ETU) model for achieving higher energy excited states using muti-photon excitation. Pumping the sensitizer center (Yb^{3+}) with 980 nm NIR light gives an ES ($^2F_{5/2}$) that can undergo energy transfer to an acceptor (Er^{3+}) to give a long lived ES. Continued excitation of the sensitizer Yb^{3+} followed by energy transfer to Er^{3+} gives the higher energy ES from which several visible range emissions occur. Figure adapted from ref. 48.

The energies of 4f-4f electronic transitions are primarily defined by spin and electronic repulsion terms and show little sensitivity to the chemical environments of the Ln^{III} cations [45]. However, 4f-4f excited state lifetimes are quite sensitive to the environment, since collisions and vibronic coupling contribute strongly to non-radiative deactivation. If an appropriate solid matrix is used, collisional contributions are eliminated and the phonon-coupling pathways are suppressed to give longer lifetimes and stronger emissions [49]. Various host crystals such as $NaGdF_4$, $NaYF_4$, $LaPO_4$, YF_3, or Y_2O_3 have been used, and the β-phase (hexagonal) $NaYF_4$ lattice has particularly favorable properties [50,51]. The large surface areas of nanoparticles exposes a sizable fraction of the lanthanoid emitters to solvent quenching, so these surface ions are protected from such environmental effects by growing a shell of the host material around the UCNP [52-54]. In addition, silica or polymer coatings can be introduced [55]. The emission properties of a Yb^{3+}/Er^{3+} nanomaterial is illustrated in Figure 7. The narrow line and long lifetime luminescence as well as the photostability of such UCNPs make them well suited for biological imaging.

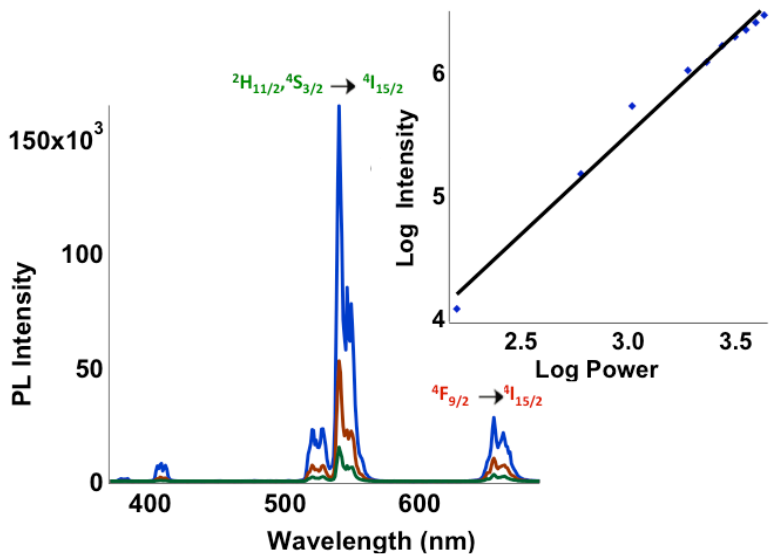

Figure 7. Upconversion emission spectra silica coated UCNPs, Yb/Er (20/2%) in β–$NaYF_4$ core with a $NaYF_4$ shell in aqueous solution. The spectra resulting from three different powers (0.58, 0.96 and 1.36 W) of a 980 nm diode laser excitation source indicate a non-linear response of emission intensity to excitation power. A log/log plot of emission intensity at 550 nm vs. power is linear with a slope of 1.63.

There have been limited studies with regard to using NIR excitation of UCNPs for uncaging reactions. Several years ago Carling et al. [56] showed that 980 nm photolysis of $NaYF_4$:Yb/Tm (30/0.5%) nanoparticles surface loaded with 3',5'-(carboxymethoxy)benzoin acetate (CBA) led

to cleavage (uncaging) of acetate from this UV absorbing organic chromophore. Similarly, Y. Yang et al. [57] utilized upconverted Tm^{3+} UV emission from $NaYF_4$:Yb/Tm (20/0.2%):$NaYF_4$ *core:shell* UCNPs to release d-luciferin conjugated to a thiolated silica layer in C6 glioma cells and in living mice. The latter experiment demonstrates how NIR excitation of UNCPs might be used to deliver bioactive molecules to living systems.

We have recently shown [58] that NIR excitation of assemblies based on $NaYF_4$:Yb/Er(20/2%):$NaYF_4$ core:shell UCNPs can trigger NO uncaging from Roussin's black salt anion $Fe_4S_3(NO)_7^-$ (RBS, Na^+ salt). Solutions of RBS alone are photoactive under UV/visible excitation (eq. 6) [59,60] but are not affected by NIR irradiation. Notably the strong

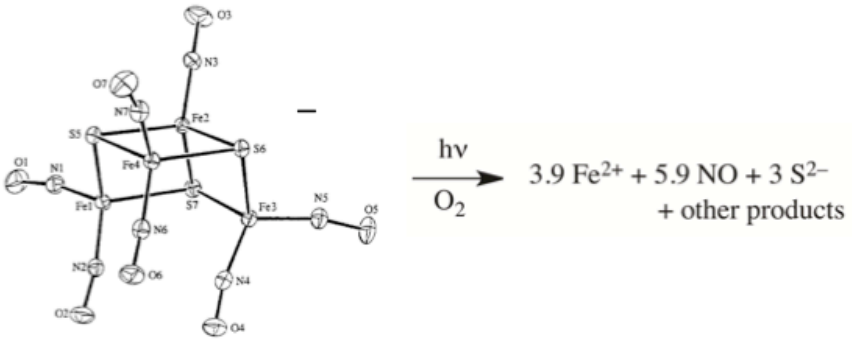

(6)

absorption bands of RBS overlay the visible range emissions of β–$NaYF_4$:Yb/Er UCNPs. Two RBS/UCNP combinations were prepared. One involved β–$NaYF_4$:Yb/Er (20/2%):$NaYF_4$ core:shell UCNPs (average diameter 20 nm) coated with a silica layer (~10 nm) surface modified with cationic -NH_3^+ groups to attract the **RBS** anions. NIR (980 nm) irradiation of these suspended in a solution of Na**RBS** resulted in the NO generation as detected by a GE Nitric Oxide Analyzer (NOA). NO output was linear with the irradiation time at constant power but showed a non-linear response to systematic increases in laser power from 1 to 4.5 W as expected.

The second approach is illustrated in Scheme 7. A mesoporous silica layer was added to the analogous UCNPs to give nanomaterials with a porous layer. These were then impregnated with RBS after which they were coated with poly(allylamine hydrochloride). The RBS remained encapsulated after washing and isolating these nanocarriers of caged NO. However, NIR irradiation released NO [58]. The quantum efficiencies for both systems were small, owing to the low photoreactivity of RBS and the low upconversion yield. Nonetheless, these proof-of-concept experiments show that UCNPs offer the opportunity to deliver NO to specific targets

using NIR light generated by a relatively inexpensive diode laser. One can anticipate that the photonic efficiencies will be improved, especially in the context that these nanocarriers offer the opportunity for targeted uncaging of NO at therapeutically relevant sites [51].

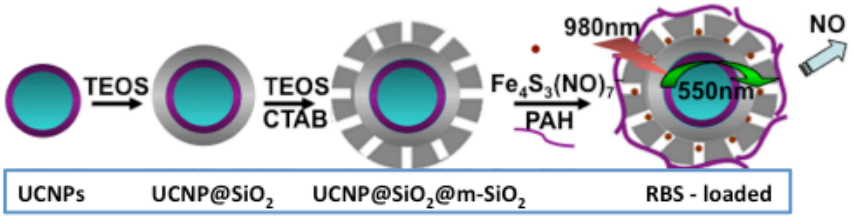

Scheme 7. Preparation UCNPs with a mesoporous silica shell impregnated with Roussin's Black Salt (red dots), a photo active nitric oxide generator, and coated with poly(allylamine). NIR irradiation leads to upconversion to wavelengths overlapping the **RBS** absorbance and NO uncaging (adapted from ref. 58)

Summary:

This article has largely summarized studies at UCSB that have explored strategies for photochemical uncaging of the nitric oxide for potential therapeutic applications. Described are studies with NO precursors coupled to antennas consisting of organic dyes or nanoparticles and utilizing both single and multiple photon excitation. The latter type of excitation offers the opportunity to use near-infrared light to access excited states that would otherwise require visible or ultraviolet light. NIR wavelengths are less damaging and will penetrate more deeply into mammalian tissue. The other advantage of multi-photon excitation is the non-linear intensity response of the induced photochemistry that offers the opportunity for three-dimensional resolution. The use of lanthanoid ion doped upconverting nanoparticles as sensitizers for NIR uncaging appears particularly promising given that physiologically relevant concentrations of NO can be uncaged using a continuous NIR diode lasers. The relatively low expense and the ease of operation and maintenance of such lasers would provide considerably greater access than the ultrafast pulsed lasers that were used to generate the intensities needed for simultaneous two photon excitation. Nonetheless, it is clear that moving any such methods from the laboratory benchtop to therapy will be very challenging.

Acknowledgement: The studies described here have received long-term support from the Chemistry Division of the US National Science Foundation (current grant CHE-1058794). I thank the many graduate, undergraduate and postdoctoral scholars and collaborators who contributed to this research.

References:

[1] P. C. Ford, J. Bourassa, B. Lee, I. Lorkovic, K. Miranda, L. Laverman, Coord. Chem. Rev. **171** (1998) 185-202.

[2] A. D. Ostrowski, P. C. Ford, Dalton Trans (2009) 10660-10669.

[3] P. C. Ford, Acc. Chem. Res. **41** (2008) 190-200.

[4] R. D. Rimmer, H. Richter, P. C. Ford, Inorg. Chem. **49** (2010) 1180 –1185.

[5] R. D. Rimmer, A. Pierri, P. C. Ford Coord. Chem. Rev., **256**, (2012) 1509-1519.

[6] A. E. Pierri, A. Pallaoro, G. Wu, P. C. Ford, J. Am. Chem. Soc. **134** (2012) 18197-18200.

[7] L.R. Makings, R. Y. Tsien, , J. Biol. Chem**. 269** (1994) 6282-6285.

[8] E. Tfouni, M. Krieger, B. R. McGarvey, D. W. Franco, Coord. Chem. Rev **236** (2003) 57-69.

[9] C. N. Lunardi, A. L. Cacciari, R. S. Silva, L. M. Bendhack, Nitric Oxide **15** (2006) 252-258.

[10] M. J. Rose, P. K. Mascharak, Coord. Chem. Rev. **252 (**2008) 2093-2114.

[11] S. Sortino, Chem. Soc. Rev. **39** (2010) 2903-2913.

[12] E. Tfouni, F. G. Doro, A. J. Gomes, R. S. da Silva, G. Metzker, P. G. Zanichelli Benini, D. W. Franco, Coord. Chem. Rev. **254 (**2010) 355-371.

[13] U. Schatzschneider, Inorg. Chim. Acta **374** (2011), 19-23.

[14] C. C. Romao, W. A. Blaettler, J. D. Seixas, Chem. Soc. Rev. **41** (2012) 3571-3583.

[15] K. L. Ciesienski, K. J. Franz. Angew. Chem. Int. Ed. **50** (2011**)** 814-824.

[16] L. A. Ridnour, D. D. Thomas, C. Switzer, W. Flores-Santana, J. S. Isenburg, S. Ambs, D. D. Roberts, D. A. Wink Nitric Oxide **19** (2008) 73-76.

[17] J. B. Mitchell, D. A., Wink, W. DeGraff, J. Gamson, L. K. Keefer, M. C. Krishna, Cancer Res., **53** (1993) 5845-5848.

[18] H. Yasuda, Nitric Oxide **19** (2008) 205-216

[19] T. C. Bellamy, C. Griffiths, J. Garthwaite, J. Biol. Chem. **277** (2002) 31801-31807.

[20] J. Bourassa, W. DeGraff, S. Kudo, D. A. Wink, J. B. Mitchell, P. C. Ford, J. Am. Chem. Soc. **119** (1997) 2853-2862.

[21] R. Motterlini, A. Gonzales, R. Foresti, J. E. Clark, C. J. Green, R. M. Winslow, Circ. Res. **83** (1998), 568-577.

[22] L. E. Otterbein, B. S. Zuckerbraun, M. Haga, F. Liu, R. P. Song, A. Usheva, C. Stachulak, N. Bodyak, R. N. Smith, E. Csizmadia, S. Tyagi, Y. Akamatsu, R. J. Flavell, T. R. Billiar, E. Tzeng, F. H. Bach, A. M. K. Choi, M. P. Soares, Nature Med**. 9** (2003) 183-190.

[23] R. Motterlini, L. E. Otterbein, Nature Rev. Drug Discovery **9** (2010) 728-743

[24] K. Katada, A. Bihari, S. Mizuguchi, N. Yoshida, T. Yoshikawa, D. D. Fraser, R. F. Potter, G. Cepinskas, Inflammation **33** (2010) 92-100.

[25] Y. Caumartin, J. Stephen, J. P. Deng, D. Lian, Z. Lan, W. Liu, B. Garcia, A. M. Jevnikar, H. Wang, G. Cepinskas, P. P. W. Luke, Kidney Int. **79** (2011) 1080-1089

[26] A. M. Smith, M. C. Mancini, S. Nie, Nature Nanotech. **4** (2009) 710-711.

[27] C. F. Works, P. C. Ford, J. Am. Chem. Soc. **122** (2000) 7592-7593.

[28] M. De Leo, P. C. Ford, J. Am. Chem. Soc. **121** (1999) 1980-1981.

[29] C. L. Conrado, J. L. Bourassa, C. Egler, S. Wecksler, P. C. Ford, Inorg. Chem., **42** (2003) 2288-2293.

[30] C. L. Conrado, S. R. Wecksler, C. Egler, D. Magde, P. C. Ford, Inorg. Chem., , **43** (2004) 5543-5549.

[31] S. R. Wecksler, A. Mikhailovsky, D. Korystov, P. C. Ford, J. Am. Chem. Soc., **128** (2006) 3831-3837.

[32] A. D. Ostrowski, R. O. Absalonson, M. A. DeLeo, G. Wu, J. G. Pavlovich, J. Adamson, B. Azhar, A. V. Iretskii, I. L. Megson, P. C. Ford, Inorg. Chem. **50** (2011) 4453-4462.

[33] A. D. Ostrowski, S. J. Deakin, B. Azhar, T. W. Miller, N. Franco, M. M. Cherney, A. J. Lee, J. N. Burstyn, J. M. Fukuto, I. L. Megson, P. C. Ford J. Med. Chem. **53** (2009) 715-722.

[34] F. DeRosa, X. Bu, P. C. Ford Inorg. Chem. **44** (2005) 4157-4165.

[35] D. Neuman, A. D. Ostrowski, A. A. Mikhailovsky, R. O. Absalonson, G. F. Strouse, P. C. Ford J. Am. Chem. Soc. **130** (2008) 168-175.

[36] P. T. Burks, A. D. Ostrowski, A. A. Mikhailovsky, E. M. Chan, P. S. Wagenknecht and P. C. Ford J. Am. Chem. Soc. **134** (2012) .

[37] W. Denk, J. H. Strickler, W. W. Webb, Science **248** (1990) 73-76.

[38] P. T. C. So, C. Y. Dong, B. R. Masters, K. M Berland, Annu. Rev. Biomed. Eng. **2 (**2000) 399-429.

[39] B. W. Pedersen, T. Breitenbach, R. W. Redmond, P. R. Ogilby. Free Rad. Res. **44** (2010) 1383-1397.

[40] G. S. He, L.-S. Tan, Q. Zheng, P. N. Prasad, Chem. Revs. **108** (2008) 1245-1330.

[41] M. Rumi, S. Barlow, J. Wang, J. W. Perry, S. R. Marder, Adv Polym Sci. **213** (2008) 1–95.

[42] S. Dayal, S., C. Burda, C. J. Amer. Chem. Soc. **130** (2008) 2890-2891.

[43] Y. Liu, P. Chen, Z. H. Wang, F. Bian, L. Lin, S. J. Chang, G. G. Mu, Laser Physics, **19** (2009) 1886-1890.

[44] S. Wecksler, A. Mikhailovsky, P. C. Ford, P. C. J. Amer. Chem. Soc**. 126** (2004) 13566-13567.

[45] S. Wecksler, A. Mikhailovsky, D. Korystov, F. Buller, R. Kannan, L.-S. Tan, P. C. Ford, Inorg. Chem. **46** (2007) 395-402.

[46] Q. Zheng, A. Bonoiu, T. Y. Ohulchanskyy, G. S He, P. N. Prasad, Mol. Pharm. **5** (2008) 389-98.

[47] S. V. Eliseeva, J.-C. G. Bunzli, Chem. Soc. Rev**. 39** (2010) 189-227.

[48] F. Zhang, Y. Wan, T. Yu, F. Q. Zhang, Y. Shi, S. Xie, Y. Li, L. Xu, B. Tu, D. Y. Zhao, Angew. Chem. Int. Ed. **46** (2007) 7976-7979.

[49] F. Wang, X. Liu, Chem. Soc. Rev. **38** (2009) 976-89.

[50] X. Wang, J. Zhuang, Q. Peng, Y. Li,. Nature **437** (2005) 121-214.

[51] G. S. Yi, G. M. Chow, Adv. Funct. Mater. **16** (2006) 2324–2329.

[52] A. D. Ostrowski, E. M. Chan, D. J. Gargas, E. M. Katz, G. Han, P. J. Schuck, D. J. Milliron, B. E. Cohen, ACS Nano **6** (2012) 2686–2692.

[53] F. Wang, J. Wang, X. Liu, Angew. Chem. Int. Ed. **49** (2010) 7456 –7460.

[54] G.-S. Yi, G.-M Chow, Chem. Mater. **19** (2007) 341–343.

[55] H. S. Qian, H. C. Guo, P. C. L. Ho, R. Mahendran, Y. Zhang, small **5** (2009) 2285–2290.

[56] C. J. Carling, F. Nourmohammadian, J. C. Boyer, N. R. Branda, Angew. Chem. Int. Ed. **49** (2010) 3782 –3785.

[57] Y. Yang, Q. Shao, R. Deng, C. Wang, X. Teng, K. Cheng, Z. Cheng, L. Huang, Z. Liu, X. Liu, B. Xing, Angew. Chem. Int. Ed. **51** (2012) 3125 –3129.

[58] J. V. Garcia, J. Yang, D. Shen, C. Yao, X. Li, G. D. Stucky, D. Y. Zhao, P. C. Ford, F. Zhang, Small, **8** (2012) 3800–3805

[59] F. W. Flitney, I. L. Megson, J. L. M. Thomson, G. D. Kennovin, A. R. Butler, Br. J. Pharmacol., **117** (1996) 1549-1557.

[60] J. L. Bourassa, B. Lee, S. Bernard, J. Schoonover, P. C. Ford, Inorg. Chem. **38** (1999) 2947-2952.